Theoretical Study of the Dissociative Adsorption of Methane on Ir(111): The Role of Steps and Surface Distortions at High Temperatures

Raquel Moiraghi,[1] Ariel Lozano,[2,3,1] and H. Fabio Busnengo[1]
[1)] *Grupo de Fisicoquímica en Interfases y Nanoestructuras, Instituto de Física Rosario and Universidad Nacional de Rosario, Bv. 27 de Febrero 210 bis, 2000 Rosario, Argentina*
[2)] *Basque Center for Applied Mathematics, Alameda de Mazarredo 14 (48009) Bilbao, Bizkaia, Spain*
[3)] *CIC EnergiGUNE, Albert Einstein 48, (01510) Miñano, Álava, Spain*

In this work we revisit the dissociative adsorption of methane on Ir(111) through Density Functional Theory calculations. We focus on the role of surface defects entailing undercoordinated Ir atoms (e.g. steps), and thermally induced distortions of a defect-free terrace. Though both factors provoke a significant activation of the $CH_3 \cdots H$ bond cleavage, our results indicate that the latter (surface distortions) is more likely the responsible for the low activation energy derived from experiments at high-surface-temperature (T_s = 1000 K) and low impact energy molecules ($E_i \lesssim 0.15$ eV). Still, since surface distortions are strongly attenuated when T_s decreases, dissociation on undercordinated Ir atoms could play a more important role for low surface temperatures. Hence, we provide useful information to guide new experiments intended to unravel the origin of the dominant dissociation pathway for low kinetic energy molecules.

I. INTRODUCTION

The dissociative adsorption of methane on transition metal surfaces is of great practical interest because it is the rate-limiting step of the catalytic steam reforming process used to produce commercial molecular hydrogen (see *e.g.* 1 and references therein). In addition, a large number of results available from well-controlled molecular beam experiments (see *e.g.* refs. 2–4) on one hand, and Density Functional Theory (DFT) (see *e.g.* refs. 5–8) and molecular dynamics (MD) (see *e.g.* refs. 9–12) calculations on the other, makes of methane/metal systems, ideal benchmarks for a deep understanding of the reactivity of polyatomic molecules on surfaces.

Molecular beam experiments have been used to investigate the reactive sticking of methane on many low-Miller-index surfaces of metallic single crystals, *e.g.*, W, Ru, Ni, Pd, Pt, and Ir[2–4,13,14]. The common main signature observed in the experiments is a strong increase (up to four orders of magnitude) of the sticking probability (S_0) with increasing normal impact energy, E_i, in the range 0.2 eV $\lesssim E_i \lesssim$ 1.2 eV. This behavior is ascribed to a direct activated mechanism governing the $CH_3 \cdots H$ bond cleavage. In such a high kinetic energy regime, methane molecules are not likely to be efficiently reoriented and/or focused by the interaction potential towards the most reactive configurations. Hence, a molecule dissociates (directly) if it hits the surface with translational energy high enough to overcome the activation barrier corresponding to the impact site and its initial orientation, being otherwise scattered back to vacuum. Thus, the sharp increase of S_0 with increasing E_i mentioned above simply reflects the increasing fraction of molecular configurations allowing dissociation.

Among the many metal surfaces used in supersonic molecular beam experiments, for some of them there is also evidence of a different reaction mechanism operative for $E_i \lesssim 0.15$ eV. This is the case of Pt(110), Ir(110), and Ir(111) for which, in such a low energy range, S_0 increases when E_i decreases. This behavior is usually considered as a fingerprint of trapping-mediated dissociation, since the trapping probability increases when E_i decreases. This is because as lower the molecular kinetic energy is, less energy redistribution between the molecular degrees of freedom (DOF) and/or energy transfer to the surface is required for the molecule to get trapped near the surface. Temporarily trapped molecules can explore a larger set of surface sites (including surface defects like steps) with many different orientations and so, can dissociate with a higher probability than in a single collision. In such a case, trapping acts as a precursor for dissociation[15].

For CH_4/Ir(111), two experimental groups independently obtained very similar sticking curves $S_0(E_i)$ pointing to precursor mediated dissociative adsorption at low impact energies[13,14]. Combining molecular beam and bulb experiments, Seets *et* al. determined an apparent activation energy of 0.28 eV for the low kinetic energy regime $E_i \lesssim 0.15$ eV[13]. Following the latter work, Dombrowski *et* al. rationalized the low energy part of the $S_0(E_i)$ sticking curve through a model considering chemisorption and desorption from a physisorbed precursor state and an activation energy for dissociation of 0.213 eV (with respect to the energy level of the molecule in vacuum)[14]. In addition, they also fitted the high energy part of the sticking curve with an *erf*-function and obtained an apparent average activation energy for direct dissociation of 1.18 eV[14]. The large ($\sim$ 1 eV) difference between apparent activation energies deduced from the low and high energy parts of the $S_0(E_i)$ curve is certainly intriguing, as well as the fact that for an impact energy of 0.5 eV (almost twice the value of the apparent activation energy estimated from the low energy regime), S_0 is as low as 0.01. This might be due to a low energy but very tight transition state (TS) as found in the past for N_2 interacting with W(110)[16] and Ru(0001)[17]. Thus,

a precise characterization of the methane/Ir(111) potential energy surface (PES) is highly desirable, in particular for future dynamical studies of reactive sticking near the threshold where not only classical over-the-barrier but also quantum tunneling can play an important role[18?] .

To our knowledge, Henkelman and Jónsson[5] were the first to compute the activation energy for the $CH_3 \cdots H$ bond cleavage on Ir(111) using DFT, and obtained $E_b \sim$ 0.3 eV, which was considered consistent with the activation energy estimated by Seets *et* al. from their low E_i-regime experimental results. However, the authors later commented that such a low DFT E_b-value was due to limitations of the k-point sampling, and that the converged barrier is approximately 0.7 eV (see ref. 28 of ref. 19). More recently, Qi *et* al.[8] also used DFT to evaluate E_b and obtained an even larger value: 0.93 eV. Thus, to date, the origin of the low ($\sim$ 0.3 eV) apparent activation energy for chemisorption extracted from experiments in the low E_i-regime remains unclear. On the one hand, a low concentration of undercoordinated Ir atoms in surface defects like steps (expected to be more reactive than those in a perfect flat Ir(111) terrace) might be playing some role in the low E_i-regime for which the reactive sticking probability is as small as $\sim 10^{-4}$[13,14]. On the other hand, thermally induced surface distortions might be affecting the results reported in refs. 13,14, obtained for a surface temperature, T_s = 1000 K. To our knowledge, none of these effects has been so far investigated theoretically and so, the aim of this work is to fill this gap. Therefore, in this paper we revisit the energetics of dissociative adsorption of methane on Ir(111) through DFT calculations. In contrast with previous investigations[5,8], here we consider not only the case of an *ideal* (flat) Ir(111) terrace in the limit of very low temperatures, but also the possible effect on the surface reactivity of: i) undercoordinated Ir atoms in steps, and ii) thermally induced *distortions* for T_s = 1000 K.

II. COMPUTATIONAL DETAILS

All the DFT calculations were performed within the generalized gradient approximation (GGA) proposed by Perdew, Burke and Ernzerhof (PBE)[20] to describe electronic exchange and correlation, and using the projector augmented wave (PAW) method[21] implemented in the plane-wave code VASP[22–26]. The energy cutoff was set in 450 eV. Electronic smearing was introduced within the Methfessel-Paxton method[27] with N=1 and σ= 0.2 eV, but all the energies informed were obtained by extrapolation to 0 K. The resulting optimum lattice parameter for Ir bulk was 3.873 Å, which agrees well with the experimental value: 3.839 Å[28].

The Ir(111) surface was modeled by a five-layer slab leaving a $\sim$ 27 Å thick vacuum space to avoid interaction with its periodic images and dipole corrections were not introduced. All the calculations were carried out for a 3×3 unit cell, and the Brillouin zone was sampled with a 5×5×1 k-point mesh using the Monkhorst-Pack method[29]. The geometry of the clean surface was optimized by allowing to relax all the Ir atoms in the two topmost layers of the slab while keeping the interlayer distance between the three bottom layers fixed to the value corresponding to Ir bulk. In geometry optimizations, the calculations were stopped when the forces on all the *mobile* atoms were smaller than 0.01 eV/Å.

To investigate the interaction energy of H, CH_3 and CH_4 species with Ir(111), the coordinates of all the Ir atoms in the two topmost layers of the slab, and those of the adsorbates have been optimized unless otherwise stated. Adsorption energies (E_{ads}) of H and CH_3 were computed using the formula:

$$E_{ads} = E[X/Ir(111)] - E[Ir(111)] - E[X] \qquad (1)$$

with X = H, or CH_3; and $E[X/Ir(111)]$, $E[Ir(111)]$, and $E[X]$ being the total energy of the $X/Ir(111)$ system, the clean Ir(111), and the X species in vacuum respectively. All the calculations except those of $E[H]$, and $E[CH_3]$, were carried out without considering spin polarization. According to Eq. 1, negative E_{ads} values correspond to exothermic adsorption.

The search for saddle points (SPs) of the CH_4/Ir(111) PES (*i*.e. transition states, TSs) corresponding to the first C-H bond cleavage process was performed in two steps: (i) first, climbing image nudged elastic band (CINEB) calculations[30] were performed until the forces on all the *mobile* atoms in the highest energy configuration were $\lesssim$ 0.06 eV/Å; (ii) then, the geometry of the highest energy configuration obtained in step (i) was optimized using the Quasi-Newton method implemented in VASP, until the forces on all the *mobile* atoms were $\leq$ 0.01 eV/Å. We have used this two-step procedure (with a *loose* stopping criterion in the first step and a stringent one in the second step) to reduce the computational cost of the CINEB calculations. The search for SPs of the PES were performed keeping the positions of all the Ir atoms fixed in their equilibrium values for the clean slab (rigid surface calculation), and also allowing the Ir atoms in the two topmost layers to relax (relaxed surface calculation). The true SP character of all the TSs geometries reported in this work has been confirmed through the calculation of the corresponding vibrational frequencies.

To investigate the reactivity of undercoordinated Ir atoms in surface defects which can never be totally avoided in experiments, we have performed calculations by removing one row of topmost layer Ir atoms. Though they correspond to a missing-row like reconstructed surface, Ir atoms which are nearest neighbors (NN) to the missing row are expected to present a reactivity similar to that of atoms in step edges between large 111 terraces. Canonical (NVT) *ab*-initio molecular dynamics (AIMD) calculations for clean Ir(111) at T_s = 500 K, and 1000 K, were performed using a Langevin thermostat with a parameter γ = 29.13 ps^{-1} chosen according to Eq. 4.11 of ref. 31. The classical equations of motion were inte-

TABLE I: H adsorption energy, E_{ads}, as defined in Eq. 1 (in eV), and optimum height of the H atom with respect to the position of the topmost layer Ir atoms in the clean Ir(111) surface, z_H, (in Å).

	top	fcc	hcp
E_{ads}	-2.75	-2.71	-2.67
z_H	1.69	1.04	1.03

grated using the Verlet algorithm[32] with a time-step, Δt = 10 fs.

G.-J. Kroes has recently reviewed the possibilities and limitations of DFT-GGA calculations to predict barriers for reactions of molecules[?] . For instance, it is well known that GGA-type functionals fail to describe Van der Waals interactions and so, physisorption wells which can act as precursor state for dissociative adsorption are described poorly. However, DFT-GGA calculations (without and with dispersion corrections) performed by Henkelman and Jónsson for CH_4/Ir(111) indicate that dispersion corrections barely affect the molecule-surface PES around the TS (see Fig. 1 of ref. 5), being only important at larger molecule-surface distances. Thus, DFT-PBE calculations are suitable for our objective of finding a possible low-activation-energy transition state allowing low impact energy CH_4 molecules to dissociate on Ir(111).

III. RESULTS

A. "Ideal" Ir(111) terrace in the limit of low temperatures

In this subsection we will consider the case of an *ideal* Ir(111) terrace as expected to be encountered by methane molecules impinging the surface in the limit of very low temperatures. Under such conditions, it is reasonable to consider the lowest-energy configuration of the *clean* Ir(111) surface (rigid surface calculation), and also accounting for possible surface distortions induced only by the interaction with the impinging methane molecules (relaxed surface calculation). The latter calculations correspond to the limit cases of sudden and adiabatic evolution of the surface DOF during the molecule-surface collision respectively. The influence of surface defects, and thermally induced surface distortions at high temperatures will be considered in subsections III B and III C respectively.

1. Dissociation products: H and CH_3 adsorption

We have first investigated the adsorption of a hydrogen atom in all the high symmetry sites of Ir(111): top,

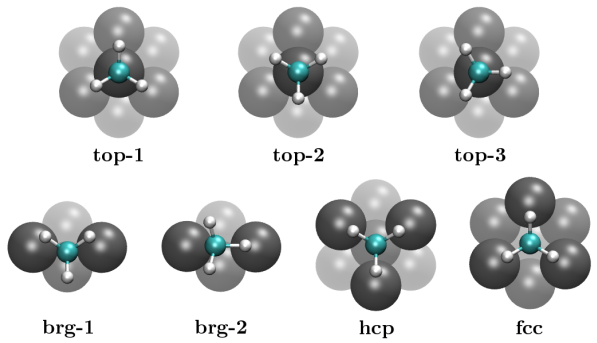

FIG. 1: Top view of the optimum configurations found for CH_3 adsorption on different sites of the Ir(111) surface[39].

bridge (brg), hollow-hcp (hcp) and hollow-fcc (fcc). In Table I we report the obtained adsorption energies and the optimum hydrogen distances to the surface, z_H, defined with respect to the height of the topmost-layer Ir atoms for the clean surface. The most stable adsorption site for hydrogen is top (E_{ads} = -2.75 eV), followed in stability by the fcc (E_{ads} = -2.71 eV) and hcp (E_{ads} = -2.67 eV) sites. We have not been able to find a stable adsorption configuration on bridge. Nevertheless, keeping fixed the lateral coordinates (x_H, y_H) of the H atom on bridge, we obtained E_{ads} = -2.66 eV, a value similar to the ones obtained for the other high-symmetry sites indicating a very low energetic corrugation of the H/Ir(111) PES. The highest stability of top sites for adsorption of H on Ir(111) is in good agreement with experiments[33–35], and the relative stability of the four high symmetry sites considered here is also consistent with previous DFT calculations[5,8,36]. The E_{ads} values reported here are slightly smaller (adsorption more stable) than those reported in ref. 36 (by between 0.02 eV and 0.17 eV), and larger (adsorption less stable) than those of ref. 5 (by between 0.13 eV and 0.17 eV). A precise comparison with the adsorption energies reported in ref. 8 is not straightforward because in the latter work, a different reference energy was used for the definition of E_{ads}. From the H_2 desorption energy extracted from Temperature Programmed Desorption (TPD) data (0.56 eV)[37], and the H_2 dissociation energy (D_0 = 4.52 eV)[38], it is possible to estimate the experimental E_{ads} value $\sim$ -2.53 eV (assuming that H_2 dissociation on Ir(111) is non-activated). This value deviates only $\sim$ 8 % from our present theoretical value and so, validates the calculation method and our particular DFT set up described above.

We have also investigated adsorption of CH_3 on the high-symmetry sites of Ir(111), and for different orientations of the C-H bonds. The final adsorption structures obtained after geometry optimization are represented in Fig. 1, and in Table II we report their corresponding E_{ads} values and the C atom height above the surface, z_C. The

TABLE II: CH_3 adsorption energy, E_{ads}, as defined in Eq. 1 (in eV), and optimum height of the C atom with respect to the position of the topmost layer Ir atoms in the clean Ir(111) surface, z_C, (in Å).

	top-1	top-2	top-3	brg-1	brg-2	hcp	fcc
E_{ads}	-1.95	-1.95	-1.94	-1.58	-1.76	-1.56	-1.66
z_C	2.26	2.26	2.26	1.89	1.92	1.71	1.69

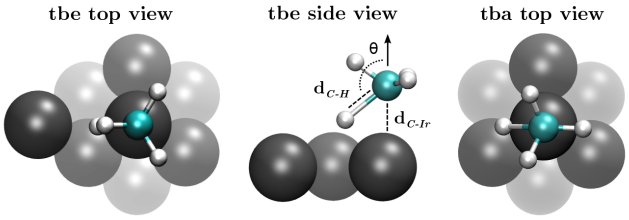

FIG. 2: Top and side views for the *tbe* (*top-bridge-eclipsed*) and top view for the *tba* (*top-bridge-alternated*) TSs configurations[39].

most stable adsorption geometries for CH_3 were found on top sites with the C-Ir bond perpendicular to the surface. In these sites we have obtained three almost isoenergetic stable structures characterized by different orientations of the C-H bonds: top-1, top-2, and top-3 (see Fig. 1). Thus, a methyl group adsorbed on a top site can rotate almost freely around the C-Ir bond. This is not surprising since for configurations with the C atom on top sites, the H atoms are far from and interact weakly with the surface. In contrast, the orientation of the C-H bonds has a stronger effect for adsorption on bridge and hollow sites. On both hcp and fcc sites, the only stable adsorption geometries found have the H atoms pointing to top sites as shown in Fig. 1. A 60° rotation of the methyl group around the C-Ir bond, provokes an energy increase of 0.45 eV. This repulsion is due to H-Ir distances shorter than in the case of adsorption on top because of the smaller optimum z_C values for methyl adsorption on hollow sites. Finally, on bridge sites we have found only two stable adsorption configurations for CH_3, brg-1 and brg-2, which significantly differ from each other in both, energy and geometry (see Fig. 1). In fact, it must be noted that the structure called brg-2, corresponds to a configuration with the C atom slightly displaced from a bridge site but still on the line joining two NN Ir surface atoms. This displacement of the C atom to a less symmetric site entails also different heights above the surface of the three H atoms, in contrast with all the other more symmetric stable structures we found.

The fact that on Ir(111), CH_3 adsorption is most stable on top sites is in agreement with DFT results reported previously[36]. The stability ordering of adsorption of CH_3 on the high-symmetry sites we have obtained, is the same as the one reported in ref. 36, being the E_{ads} values reported here slightly smaller (adsorption more stable) than those of the latter work (*e.g.* by 0.07 eV for top sites). Also, the present E_{ads} values for top sites are 0.32 eV larger (adsorption less stable) than the one reported in ref. 5. The origin of this relatively large discrepancy is very likely due to limitations in the k-point sampling used in ref. 5 as already mentioned above[19].

2. Transition states for $CH_3\cdots H$ dissociation

We have looked for the saddle points of the CH_4/Ir(111) PES corresponding to $CH_3\cdots H$ dissociation for molecular configurations with the C atom on various high-symmetry surface sites and for different orientations of the C-H bonds. To identify the various resulting SP configurations we assign to each of them a three-letter name: (i) the first letter indicates the high-symmetry surface site closest to the C atom (*t* for top, *b* for brg, *h* for hollow-hcp, and *f* for hollow-fcc sites), (ii) the second letter indicates the high-symmetry site to which the breaking C-H bond is pointing to, and (iii) the third letter indicates the relative orientation of the C-H bonds of the *intact* methyl group with respect to the breaking C-H bond (*a* for alternated, and *e* for eclipsed structures). This nomenclature is illustrated in Fig. 2 for the *tbe* (the lowest energy TS we have found, see below) and *tba* structures.

The energies of the SPs are defined with respect to a reference configuration with the CH_4 molecule and the Ir(111) surface, both in equilibrium and far from each other (for a C-surface distance of 6 Å). In this reference configuration, the C-H distances are 1.1 Å, and the H-C-H angles are 109.5°, both in good agreement with the experimental values for the *free* CH_4 molecule[38]. Table III summarizes the energies and geometries of all the SPs we have found following the procedure described in Section II in both, rigid and relaxed surface calculations. We have found six TSs with the C atom on top and one with the C atom on a bridge site (hereafter referred to as t-type and b-type TSs respectively). In both rigid and relaxed surface calculations, the lowest energy TS obtained was the *tbe*, corresponding to an eclipsed geometry with the C atom on top of an Ir atom and the breaking C-H bond pointing to a bridge site. Only one imaginary frequency has been obtained for the TSs reported in this work, except in a few cases in which we were unable to avoid some additional imaginary frequencies (very small in absolute value) probably due to small numeric errors for *flat saddle points*, e.g. the *bhe* geometry in relaxed surface calculations.

The six t-type TSs are almost isoenergetic and differ

TABLE III: TSs properties Energies are informed in eV referenced at the methane far from the slab. All distances are in Å and the z coordinates of C and Ir atoms are defined with respect to the height of the surface Ir atoms in the clean surface. The θ angle is expressed in degrees.

Name	E_b	$d_{C\text{-}H}$	$d_{C\text{-}Ir}$	z_C	z_H	z_{Ir}	θ
			Rigid Surface				
tbe	0.83	1.53	2.29	2.29	1.29	0	130.7
tba	0.84	1.50	2.31	2.31	1.29	0	132.8
the	0.85	1.55	2.28	2.28	1.25	0	131.8
tha	0.86	1.53	2.30	2.30	1.27	0	132.7
tfe	0.85	1.54	2.29	2.29	1.26	0	131.8
tfa	0.86	1.51	2.30	2.30	1.28	0	132.4
bhe	1.56	1.64	2.63	2.25	1.17	–	131.0
			Relaxed Surface				
tbe	0.66	1.50	2.26	2.42	1.42	0.17	131.9
tba	0.67	1.47	2.28	2.44	1.44	0.16	133.0
the	0.67	1.52	2.25	2.42	1.41	0.17	131.7
tha	0.68	1.49	2.27	2.44	1.44	0.17	132.1
tfe	0.68	1.52	2.25	2.42	1.41	0.16	131.6
tfa	0.69	1.49	2.27	2.44	1.44	0.17	132.1
bhe	1.42	1.59	2.59	2.26	1.09	–	137.3

from each other in the direction of the breaking C-H bond and the eclipsed and alternated character. They are all characterized by very similar values of the dissociating C-H bond length, d_{C-H} ($\sim$ 1.52 Å), and azimuthal angle, θ ($\sim$ 131°); the shortest C-Ir distance, d_{C-Ir} ($\sim$ 2.3 Å), and the heights of the *active* C, H, and Ir atoms, z_C, z_H, and z_{Ir} respectively (see Table III). These six similar E_b values for t-types TSs are not unexpected in view of the relatively weak energetic corrugation of the H/Ir(111) PES (see Table I) and the fact that the CH_3 group can rotate almost freely around the C-H bond when is adsorbed on top sites (see Table II). In addition, almost isoenergetic t-type TSs for CH_3-H dissociation have been reported also for Ni(111) and Pt(111)[7].

From Table III, it is clear that surface relaxation contributes significantly to reduce the energy of all the t-type TSs, E_b decreases *c*a. 0.17 eV when surface relaxation is allowed. This energy lowering is mainly due to a 0.16-0.17 Å shift up of the Ir atom closest to the molecule (the *active* one) with respect to its optimum position for the clean surface. If the only surface DOF optimized during the search of the *tbe* TS is the *z* coordinate of the *active* Ir atom, the resulting E_b value is only a few meV larger than the one obtained in the unconstrained geometry optimization. This surface relaxation effect is very similar to the one found for CH_4 dissociation on Ni(111) and Pt(111)[18,40–42]. Still, the *active* Ir atom shift-up is, in magnitude, the same as for Pt atoms but 0.04 Å smaller than for Ni ones, and the resulting E_b lowering for Ir(111) is $\sim$ 0.04 eV larger than the one obtained for both Ni(111) and Pt(111). We will come back to the importance of Ir atom displacements from their equilibrium positions in the CH_4/Ir(111) reactivity in Section III C.

Concerning the comparison with the activation energy barriers reported previously for CH_4/Ir(111) by other authors, the lowest value we have obtained (*i*.e. 0.66 eV for the *tbe* TS geometry, allowing surface relaxation) is in reasonably good agreement with the k-point converged value mentioned in ref. 19 (0.7 eV), and 0.27 eV smaller than the one reported by Qi *et* al.[8]: 0.93 eV. The latter significant discrepancy might be partially due to the use of a 2×2 supercell in ref. 8, which is known to entail an increase of the activation energy barrier for methane dissociation with respect to calculations performed in a 3×3 supercell due to the higher surface coverage[43].

Since vibrational softening is expected to play an important role in the C-H bond breaking process we have also computed the activation energy barrier including vibrational zero point energy (ZPE) corrections. This reduces the activation energy barrier in $\sim$ 0.1 eV; *e*.g. including ZPE corrections, for the *tbe* TS, E_b becomes equal to 0.73 eV and 0.57 eV for the rigid and the relaxed surface respectively.

Apart from the lowest energy t-type TSs described above, in Table III we also report a b-type one (*bhe*, with the C atom on a bridge site) whose energy is larger than for the t-type ones by $\sim$ 0.7 eV. In line with the rule that predicts a larger activation energy for a TS located closer to the exit channel (late TS), the d_{C-H} value of the *bhe* TS is $\sim$ 0.1 Å larger than for the t-type ones. Various attempts to find a SP with the C atom on hollow sites were unfruitful. Nevertheless, by performing the geometry optimization over a hollow-fcc site while fixing the lateral coordinates of the C atom (x_C,y_C), we have found an *activation energy barrier* of 1.72 eV for the rigid surface. Despite the latter activation energy does not correspond to a true SP of the PES, this energy value is still representative of the cost for breaking the first C-H bond if the C atom is on a hollow-fcc site. Such an energy cost on hollow-fcc sites is 0.89 eV and 0.16 eV larger than for the *tbe* and *bhe* configurations respectively. Thus, CH_4/Ir(111) can be considered as a system with a high energetic corrugation for which dissociation on top sites is energetically largely favored with respect to other surface sites. Thus, low energy CH_4 molecules are expected to dissociate only on top sites of Ir(111).

The E_b values obtained for the Ir(111) terraces are consistent with the apparent activation energy obtained experimentally for the high energy part of the sticking curve[13,14]. Nevertheless, the lowest E_b value found is considerably higher than the apparent activation energy extracted from experiments corresponding to low-energy molecules impinging Ir(111). Therefore, in the following subsections we will explore other possible reaction pathways with lower energy barriers due to the existence of

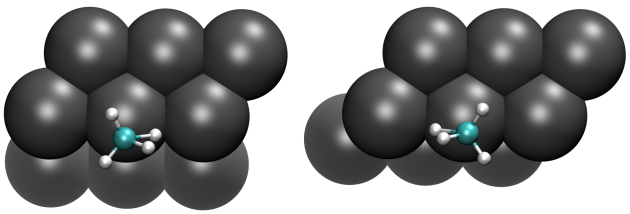

FIG. 3: Top views for the tbe TS in steps type A and B[39].

TABLE IV: Properties of the *tbe* TS on type A and B steps: Energies are informed in eV referenced at the methane far from the slab. All distances are in Å and the z coordinates of C and Ir atoms are defined with respect to the height of the surface Ir atoms in the clean surface. The θ angle is expressed in degrees.

	E_b	$d_{C\text{-}H}$	$d_{C\text{-}Ir}$	z_C	z_H	z_{Ir}	θ
step-A	0.28	1.44	2.26	2.20	1.24	0.10	131.4
step-B	0.35	1.48	2.25	2.28	1.32	0.10	130.5

surface defects like steps, and thermally induced surface distortions.

B. CH_4 dissociation on Ir(111) with monoatomic steps

It is well known that under-coordinated atoms in steps are, in general, more reactive than those located in flat terraces (see 44 and references therein). In addition, when dealing with flat low Miller index metal surfaces, in practice it is not possible to completely avoid steps. Thus, whenever a surface-reaction probability is smaller than or similar to the fraction of surface atoms near defects, steps are potential candidates to dominate the observed reactivity. This is so in particular, for low impact energy molecules which are more likely to get trapped, explore a large surface area and encounter a step-edge. These conditions are certainly met in the case of CH_4/Ir(111). For $E_i \lesssim 0.3$ eV, the sticking probabilities reported (for $T_s = 1000$ K) are $\sim 10^{-4}$ and the fraction of defect sites is estimated to be less than 5×10^{-3}[13]. In addition, trapping of low energy molecules has been identified both experimentally,[13] and in MD simulations[?] that predicted, *e.g.*, a trapping probability of ~ 0.4 in a wide range of temperatures (between 50 K and 1500 K) and a lifetime of the trapped molecules as long as ~ 9 ps for $E_i = 50$ meV.

In this context, it is important to estimate in what extent steps might influence the reactivity of the Ir(111) surface for methane dissociative adsorption. Therefore, we have carried out DFT calculations for two model step-edges of Ir(111), usually called type-A and type-B steps. They are characterized by {100} and {111} microfacets respectively (see Fig. 3) and for Ir(111), type-B steps are expected to be more stable, and so more abundant than type-A ones[45]. The lowest energy TS geometry obtained for the flat surface (*tbe*) was used as starting point for the search of the TSs on both step-edges and the geometry optimization was performed allowing the relaxation of the Ir atoms in the two topmost layers. The resulting TS geometries are shown in Fig. 3. During the optimization, the methane molecule shifted from the initial *tbe* configuration displayed in Fig. 2 towards the step-edge. On the type-A and type-B steps we have respectively found E_b values equal to 0.28 eV and 0.35 eV, and $d_{C\text{-}H}$ values 0.06 Å and 0.03 Å shorter than for the *tbe* TS on the terrace (see Table IV). Thus, near both step-edges the activation energy barrier becomes smaller and earlier than in the perfect Ir(111) terrace. As expected, the lowest activation energy barrier was found for the predicted less stable step-edge. For the most stable type-B step, the barrier for methane dissociation is 0.31 eV lower than on a perfect terrace. A very similar activation energy reduction has been also obtained in a test calculation of the TS on a B-type step modeled using a 3×6 supercell and removing three topmost-layer Ir rows, which entails a distance between consecutive steps twice larger than in the calculations in the 3×3 supercell (9.8 Å vs. 4.9 Å). This validates our model calculations used to estimate the reactivity of Ir atoms near a step-edge of Ir(111). Interestingly, the 0.35 eV activation energy barrier on type-B steps is not far from the activation energy estimated from experimental data for the low energy regime[13,14]. These low energy barriers support the hypothesis of trapping followed by dissociation on step-edges as a possible significant mechanism for CH_4 dissociation in the low E_i-regime. Still, it must be taken into account that in general, when surface defects become dominant, reactivity measurements tend to be less reproducible since the density of steps might vary from one sample to the other, and so depend strongly on the surface preparation method. Since for CH_4/Ir(111), two experimental groups have obtained (independently) initial sticking probabilities very similar to each other, it seems also reasonable to argue that these measured reactivities should be mostly due to dissociative adsorption on terraces[13,14]. In addition, the activation energy barriers for methane dissociation on perfect Ir(111) and Pt(111) terraces are very close to each other[46], as well as the ones we have obtained on top of undercoordinated atoms in step-edges. Then, this can be considered as another possible argument against steps as the main responsible for a low-activation-energy dissociation pathway on Ir(111) since otherwise, a similar low-energy mechanism should be observed for Pt(111) (where steps are presumably also present) but this has not been reported so far. In this context, it is worth to explore other possible low-activation-energy pathways

for CH_4 dissociation on Ir(111) in the low energy regime.

C. Role of lattice distortions at high temperatures

The molecular beam experimental data reported in refs. 13,14 were obtained for surface temperatures between 700 K and 1000 K. At such high temperatures the typical instantaneous displacements of the metal atoms with respect to their equilibrium positions can be large. Thus, the surface structure encountered by the impinging molecules for $T_s \sim 1000$ K, can differ substantially from that used in our rigid surface calculations. Moreover, the large difference between the TS energies obtained for rigid- and relaxed-surface calculations (see Section III A 2) suggest that thermally induced distortions of the Ir(111) surface might affect significantly the activation barrier for $CH_3 \cdots H$ dissociation. The aim of this subsection is to explore this in more detail. Due to the mass mismatch between methane and Ir atoms, the effect on reactive sticking of the coupling between molecular and surface DOF during the molecule-surface collision is expected to be weak. This has been recently confirmed for CH_4/Pt(111) by classical trajectory calculations using a Static Distorted Surface (SDS) model. In contrast with standard classical trajectory calculations where both molecular and surface DOF evolve during the collision process, in the SDS model the surface atoms are kept fixed in their initial positions, chosen according to the surface temperature of interest[46]. Thus, within the SDS model (*i*.e. a sudden approximation for the surface DOFs), surface temperature influences the probability for a molecule of encountering a given distorted surface configuration but not the dynamical coupling between molecular and surface DOFs whose effect is totally neglected. In spite of this, SDS and standard classical trajectory calculations give very similar reactive sticking probabilities of CH_4 on Pt(111)[46].

The validity of the SDS model motivated us to perform molecular geometry optimizations to look for additional TSs for $CH_3 \cdots H$ dissociation on fixed distorted configurations of the Ir(111) surface. From the results described in Section III A 2, a natural choice of possible distorted surface configurations consists in displacing an Ir atom in the direction perpendicular to the surface, z, and keeping all the others fixed in their equilibrium positions for the clean surface (this will be hereafter referred to as the *one-displaced-atom*, ODA, model). Defining z_{Ir} as the magnitude of such an outward (positive z_{Ir}) or inward (negative z_{Ir}) displacement of the *active* Ir atom with respect to the other topmost-layer Ir atoms, we performed geometry optimizations of the *tbe*-like TS for z_{Ir} values between -0.3 Å and +0.5 Å (*i*.e. z_{Ir}=0 corresponds to a rigid surface calculation). The activation energies E_b obtained within the ODA model for CH_4/Ir(111) are represented in Fig. 4 with red circles. It is important to mention that in each case, the reported activation energies are defined with respect to that of the molecule in its

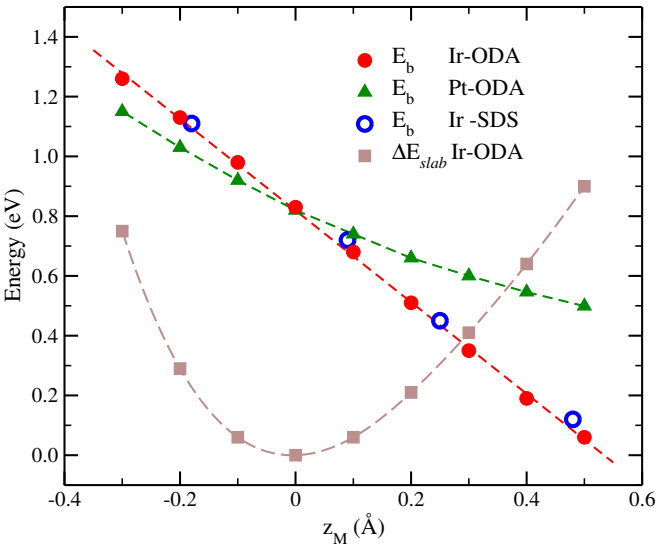

FIG. 4: Variation of the *tbe* TS energy barrier with z_M ($M = Ir, Pt$) in the: ODA model of Ir(111) (red circles and dash line, linear fit), ODA model of Pt(111) (green triangles) and SDS of Ir(111) at 1000 K (blue rings); energy ref.: methane far from the distorted slab. Brown squares: energy excess of the ODA slab relative to the equilibrium Ir(111) slab.

equilibrium configuration far form the distorted surface. Thus, the energy cost of producing the surface distortion (also represented as a function of z_{Ir}, in Fig. 4 through brown squares) is not included in the activation energies. Fig. 4 shows that E_b decreases almost linearly when z_{Ir} increases (for z_{Ir}=0, E_b=0.83 eV, *i*.e. the rigid surface value reported in Table III). A decrease of $E_b(z_{Ir})$ is not unexpected because by shifting an Ir atom up, its bounds with NN Ir atoms are weaken which is expected to turn it more reactive for an impinging molecule. However, much less predictable is the linear decrease of $E_b(z_{Ir})$ with a large negative slope (-1.5 eV/Å), even for z_{Ir} values as large as +0.5 Å. This entails a strong reduction of E_b, which becomes smaller than 0.1 eV for z_{Ir}=+0.5 Å. The latter activation energy barrier could be further lowered (by $\sim$ 0.1 eV) if ZPE corrections are taken into account turning dissociation almost a non-activated process. In order to compare this surprising behavior with other transition metal surfaces, we have performed ODA model calculations also for CH_4/Pt(111) which, for the undistorted surface, is characterized by a similar activation energy barrier. The obtained results are also represented in Fig. 4 with green triangles. Interestingly, it is observed that in the case of CH_4/Pt(111), the $E_b(z_{Pt})$ dependence is not linear and the local slope of the curve is always smaller (in absolute value) than for CH_4/Ir(111). Thus, in the case of CH_4/Pt(111), for z_{Pt}=+0.5 Å, $E_b \sim$ 0.5 eV, in strong contrast with the case of CH_4/Ir(111). Interestingly, our ODA model results for CH_4/Pt(111) are in very good agreement with those reported by Jack-

son and co-workers for a more restricted range of displacements of the active Pt atom: i.e. ± 0.2 Å(see Table V of ref. 7). Moreover, for CH_4/Ni(111) for which it has been investigated the effect of z_{Ni} variations up to ± 0.35 Å[47], it was also found a nonlinear $E_b(z_{Ni})$ dependence similar to the one we have obtained for CH_4/Pt(111). Thus, we conclude that the strong and linear decrease of $E_b(z_{Ir})$ (even for large z_{Ir} values) is not a general property of transition metal surfaces but an interesting peculiarity of CH_4/Ir(111).

Since in the ODA model only one Ir atom is displaced from its equilibrium position, it is convenient to explore to what extent the ODA model results can be linked to *real* thermal distortions. Thus, we have carried out NVT AIMD calculations for clean Ir(111) at T_s = 1000 K (*i*.e. a typical surface temperature used in the experiments)[13,14], and we have selected four different snapshots with z_{Ir} values from -0.18 Å to +0.48 Å. Since all the Ir atoms in the two outermost layers of the surface are mobile in the AIMD calculations, in this case z_{Ir} measures the average height of the *active* Ir atom with respect to its six NN topmost-layer Ir atoms. For these four configurations we have also performed molecular geometry optimizations (keeping fixed the surface DOFs) looking for a *tbe*-like TSs. The obtained E_b values are also represented in Fig. 4 with open blue circles. The obtained results for all the z_{Ir} values agree very well with those of the ODA model. This strongly suggests that the reactivity of an Ir atom is mainly determined by the relative height with respect to its NN surface atoms only. Hence, for a given distorted surface configuration (*e*.g. obtained during an AIMD run at a given temperature) the minimum activation energy barrier E_b on top of any Ir atom, can be estimated from the results of the ODA model for the same value of z_{Ir} (according with the red dashed line in Fig. 4).

The probability of finding a topmost layer Ir atom vertically displaced in z_{Ir} with respect to its six NN surface atoms for Ir(111) at T_s=500 K and T_s = 1000 K are shown in Fig. 5. These results were obtained from the NVT AIMD calculations described above. In the bottom axis, we represent the z_{Ir} values whereas in the top one, we represent the corresponding E_b values predicted by the linear relationship $E_b(z_{Ir})$ shown in Fig. 4 (red dashed line).

In Fig. 5 we have also plotted the Gaussian functions that best fit the NVT-AIMD distributions for 500 K and 1000 K. They correspond to the distribution of displacements of 1D classical harmonic oscillators of frequencies, 109 cm^{-1} and 90 cm^{-1} respectively. The former value is close to the frequency derived from the curve $\Delta E_{slab}(z_{Ir})$ shown in Fig. 4 (130 cm^{-1}), expected to be found in AIMD calculations in the limit of low surface temperatures. Moreover, the latter value is also consistent with the limit of the Ir(111) perpendicular component of the effective surface Debye temperature derived from low energy electron diffraction (LEED) experiments in the limit of small $\Delta k_\perp$ values of the scattered electrons[?] . From

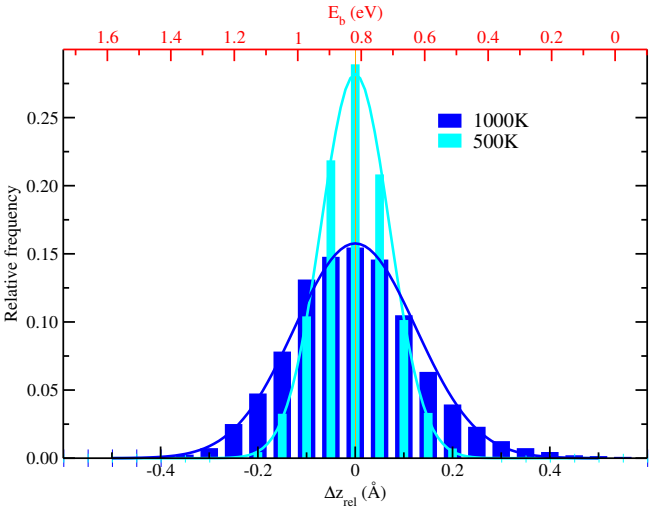

FIG. 5: Probability of finding an Ir atom displaced in z_{Ir} for Ir(111) at 500 K and 1000 K computed from AIMD calculations. In the top axis there are also the E_b values related to the z_{Ir} though the linear relationship obtained with the ODA model (see Fig. 4).

the NVT-AIMD results shown in Fig. 5 for T_s = 1000 K, the fraction of Ir atoms characterized by z_{Ir} values giving activation energies smaller than 0.35 eV (the minimum E_b value found for our model type-B step) is ∼ 0.015. This value is much larger than the typical experimental fraction of Ir atoms in steps of a Ir(111) surface, estimated to be less than 5×10^{-3}[13]. Thus, our results point to dissociation on thermally distorted terraces of Ir(111) as the responsible of the low activation energy estimated from experiments in the low E_i-regime for T_s = 1000 K[13,14]. In contrast, for T_s = 500 K, the probability of finding such a large distortion decreases a lot in spite of the fact that the relatively short integration time during our AIMD runs (*i*.e. 10 ps) prevents a precise evaluation of such infrequent events. In any case, for T_s = 500 K, it is expected that the fraction of Ir atoms with $z_{Ir} \geq 0.3$ Å is of the same order of magnitude or smaller than the typical fraction of Ir atoms in steps-edges of Ir(111) in experiments[13,14]. From the results of Figs. 4 and 5 the minimum possible activation energy barrier due to thermally induced distortions at T_s = 500 K is *c.a.* 0.5 eV. Thus, for temperatures of 500 K and below, thermally induced surface distortions are expected to be less important than steps. If the active sites in hot terraces are the main responsible for the low-impact-energy dissociation pathway and the corresponding increase in reactivity at low E_i values, our results predict that the upturn of the sticking probability observed at low impact energies would be strongly attenuated (or disappear) below ∼ 500 K. Unfortunately, to our knowledge, the low-E_i regime has not been investigated experimentally for surface temperatures below 700 K so far[13]. Finally, it is important to stress that thermally induced surface dis-

tortions near a step-edge (*i*.e. a combination of the two effects considered separately above) should be also considered for a complete analysis. However, the comparison of the relative role of both effects, *i*.e. thermally induced distortions and steps (the aim of this work) justifies our simplified (separated) approach.

IV. CONCLUSIONS

In this work we have used Density Functional Theory (DFT) calculations to investigate the energetic of the first C-H bond cleavage during methane chemisorption on Ir(111). We found that the reactivity is primarily due to transition states (TSs) with the C atom on top of an Ir atom, *i*.e t-type TSs. For an *ideal* flat terrace of Ir(111), we have found a minimum activation energy barrier E_b = 0.83 eV (0.66 eV if surface relaxation is allowed). Such a high activation energy is consistent with the apparent activation energy estimated from molecular beam results for high impact energies (above 0.15 eV) but cannot explain the low activation energy ($\sim$ 0.3 eV) estimated for low impact energies and high surface temperatures ($T_s \sim$ 1000 K). In order to explore possible reasons for this apparent contradiction between theory and experiments, we have studied the effect of: i) monoatomic steps, and ii) thermally induced surface distortions. In the former case we have obtained a transition state (TS) with E_b = 0.35 eV for the most stable step, close to the activation energy estimated from experiments for the low E_i-regime. However, we have shown through static and dynamic DFT calculations that, for T_s = 1000 K, thermally induced surface distortions also provide low-energy dissociation pathways on Ir(111) terraces. We have found that in this case, the lowering in E_b is mainly due to vertical outward displacements of the Ir atoms with respect to its nearest neighbor (NN) surface atoms. The latter pathway becomes energetically more favorable than dissociation on a step-edge for vertical shifts $z_{Ir} \gtrsim 0.3$ Å. Our *ab*-initio molecular dynamics (AIMD) calculations show that at T_s = 1000 K, the fraction of Ir atoms reaching such large vertical outward displacements is higher than the typical fraction of atoms in step-edges in the well-controlled flat closed-packed Thus, thermally induced distortions of *ideal* Ir(111) terraces are more likely to be responsible for the low activation energy pathway observed in experiments at $T_s \sim$ 1000 K. Thermal distortions dominating reactivity is also consistent with the good reproducibility of the experiments since the density of surface defects in general depends strongly on the surface preparation and cleaning procedure. In such a case, our results predict a disappearance of the low-energy channels for lower temperatures (*i*.e. $T_s \sim$ 500 K) and the consequent drop of the initial reactive sticking probability, S_0, at low impact energies. In order to unambiguously establish the precise mechanism for dissociative adsorption at low translational energies, further investigations are still needed. On the one hand, experiments involving Ir(111) surfaces with different density of steps might shed some light on the role of such defects, and a systematic study of surface temperature effects might also contribute to discard or support the role of thermally induced lattice distortions. On the other hand, MD calculations for CH_4/Ir(111) are also necessary. In particular calculations properly accounting for surface temperature effects up to 1000 K, and incorporating properly dispersion forces and the role of defects. Work in this direction is being undergone in our group.

V. ACKNOWLEDGEMENTS

The authors acknowledge Arthur Utz for providing us experimental results for CH_4/Ir(111) before publication and useful discussions, and the *CCT-Rosario* Computational Center, member of the High Performance Computing National System (SNCAD, MincyT-Argentina) for allocation of computer time. This work has been supported by ANPCyT (project PICT Bicentenario N° 1962), CONICET (project PIP 0667), and UNR (project PID ING235).

[1] J. R. Rostrup-Nielsen, J. Sehested, and J. K. Nørskov, Adv. Catal. **47**, 65 (2002).
[2] J. F. Weaver, A. F. Carlsson, and R. J. Madix, Surf. Sci. Rep. **50**, 107 (2003).
[3] L. Juurlink, D. Killelea, and A. Utz, Prog. Surf. Sci. **84**, 69 (2009).
[4] R. Beck and A. Utz, in *Dynamics of Gas-Surface Interactions*, Springer Series in Surface Sciences, Vol. 50, edited by R. Díez Muiño and H. F. Busnengo (Springer Berlin Heidelberg, 2013) Chap. 8, pp. 179–212.
[5] G. Henkelman and H. Jónsson, Phys. Rev. Lett. **86**, 664 (2001).
[6] A. T. Anghel, D. J. Wales, S. J. Jenkins, and D. A. King, Phys. Rev. B **71**, 113410 (2005).
[7] S. Nave, A. K. Tiwari, and B. Jackson, J. Chem. Phys. **132**, 054705 (2010).
[8] Q. Qi, X. Wang, L. Chen, and B. Li, App. Surf. Sci. **284**, 784 (2013).
[9] B. Jackson, in *Dynamics of Gas-Surface Interactions*, Springer Series in Surface Sciences, Vol. 50, edited by R. Díez Muiño and H. F. Busnengo (Springer Berlin Heidelberg, 2013) Chap. 9, pp. 213–237.
[10] B. Jiang, R. Liu, J. Li, D. Xie, M. Yang, and H. Guo, Chem. Sci. **4**, 3249 (2013).
[11] F. Nattino, H. Ueta, H. Chadwick, M. E. van Reijzen, R. D. Beck, B. Jackson, M. C. van Hemert, and G.-J. Kroes, J. Phys. Chem. Lett. **5**, 1294 (2014).
[12] X. J. Shen, A. Lozano, W. Dong, H. F. Busnengo, and X. H. Yan, Phys. Rev. Lett. **112**, 046101 (2014).
[13] D. C. Seets, C. T. Reeves, B. A. Ferguson, M. C. Wheeler, and C. B. Mullins, J. Chem. Phys. **107**, 10229 (1997).
[14] E. Dombrowski, E. Peterson, D. D. Sesto, and A. Utz, Catal. Today **244**, 10 (2015).
[15] H. F. Busnengo, W. Dong, and A. Salin, Phys. Rev. Lett. **93**, 236103 (2004).
[16] M. Alducin, R. Díez Muiño, H. F. Busnengo, and A. Salin, Phys. Rev. Lett. **97**, 056102 (2006).
[17] C. Díaz, J. K. Vincent, G. P. Krishnamohan, R. A. Olsen, G. J. Kroes, K. Honkala, and J. K. Nørskov, Phys. Rev. Lett. **96**, 096102 (2006).
[18] S. Nave, A. K. Tiwari, and B. Jackson, J. Phys. Chem. A **118**, 9615 (2014), http://dx.doi.org/10.1021/jp5063644.

[19]G. Henkelman, A. Arnaldsson, and H. Jónsson, J. Chem. Phys. **124**, 044706 (2006).
[20]J. P. Perdew, K. Burke, and M. Ernzerhof, Phys. Rev. Lett. **77**, 3865 (1996).
[21]P. E. Blöchl, Phys. Rev. B **50**, 17953 (1994).
[22]G. Kresse and J. Hafner, Phys. Rev. B **47**, 558 (1993).
[23]G. Kresse and J. Hafner, Phys. Rev. B **49**, 14251 (1994).
[24]G. Kresse and J. Furthmüller, Comput. Mater. Sci. **6**, 15 (1996).
[25]G. Kresse and J. Furthmüller, Phys. Rev. B **54**, 11169 (1996).
[26]G. Kresse and D. Joubert, Phys. Rev. B **59**, 1758 (1999).
[27]M. Methfessel and A. T. Paxton, Phys. Rev. B **40**, 3616 (1989).
[28]C. Kittel, *Introduction to solid state physics* (New York, John Wiley & Sons, 1971).
[29]H. J. Monkhorst and J. D. Pack, Phys. Rev. B **13**, 5188 (1976).
[30]G. Henkelman, B. Uberuaga, and H. Jónsson, J. Chem. Phys. **113**, 9901 (2000).
[31]J. C. Tully, J. Chem. Phys. **73**, 1975 (1980).
[32]L. Verlet, Phys. Rev. **165**, 201 (1968).
[33]C. J. Hagedorn, M. J. Weiss, and W. H. Weinberg, Phys. Rev. B **60**, R14016 (1999).
[34]M.-S. Liao and Q.-E. Zhang, J. Mol. Catal. A-Chem. **136**, 185 (1998).
[35]C.-T. Au, C.-F. Ng, and M.-S. Liao, J. Catal. **185**, 12 (1999).
[36]W. P. Krekelberg, J. Greeley, and M. Mavrikakis, J. Phys. Chem. B **108**, 987 (2004).
[37]J. R. Engstrom, W. Tsai, and W. H. Weinberg, J. Chem. Phys. **87**, 3104 (1987).
[38]D. R. Lide, *CRC Handbook of Chemistry and Physics 2003-2004* (CRC Press: Boca Raton, FL, 2003).
[39] This image was made with VMD. VMD is developed with NIH support by the Theoretical and Computational Biophysics group at the Beckman Institute, University of Illinois at Urbana-Champaign.
[40]S. Nave and B. Jackson, Phys. Rev. Lett. **98**, 173003 (2007).
[41]S. Nave and B. Jackson, J. Chem. Phys. **130**, 054701 (2009).
[42]A. K. Tiwari, S. Nave, and B. Jackson, Phys. Rev. Lett. **103**, 253201 (2009).
[43]H. Ueta, L. Chen, R. D. Beck, I. Colon-Diaz, and B. Jackson, Phys. Chem. Chem. Phys. **15**, 20526 (2013).
[44]B. Hammer, Top. Catal. **37**, 3 (2006).
[45]S. Papadia, M. C. Desjonquères, and D. Spanjaard, Phys. Rev. B **53**, 4083 (1996).
[46]A. Lozano, X. Shen, R. Moiraghi, W. Dong, and H. Busnengo, Surf. Sci. **640**, 25 (2015).
[47]X. Shen, Z. Zhang, and D. H. Zhang, Phys. Chem. Chem. Phys. **17**, 25499 (2015).